Annual Progress Report for JFY 2002

April 25, 2003

CDF Experiment

Spokespersons
Japan S. Kim (University of Tsukuba)
U.S.A. A. T. Goshaw (Duke University), N. S. Lockyer (University of Pennsylvania)

The year 2002 was the second year of the Tevatron Run-II program and the CDF experiment. Run II officially started in March 2001. Tevatron accelerator has been running smoothly, now with 36 bunches of protons and anti-protons, respectively, at an increased center-of-mass energy of almost 2 TeV. Thus far a peak luminosity of $\mathcal{L} = 4.1 \times 10^{31}$ cm^{-2} s^{-1} has been achieved (Figure 1(top)). This is more than twice as high as the best value achieved in Run I. A weekly integrated luminosity in excess of 7 pb^{-1} and a total integrated luminosity of over 200 pb^{-1} have been delivered to the experiments (Figure 1(bottom)).

And throughout 2002 the CDF experiment accumulated collision data steadily. The upgraded CDF detector has been functioning very well with high efficiency. The integrated luminosity recorded by CDF amounts to roughly 160 pb^{-1}, surpassing the amount recorded in Run I (Figure 2). We expect the instantaneous luminosity value to improve further over the next several months, and expect to accumulate about a few hundred pb^{-1} of data by the end of this year. The Tevatron Run IIa, scheduled through 2004, should deliver a total integrated luminosity of 2 fb^{-1} to CDF. After that, in Run IIb, an instantaneous luminosity of 4×10^{32} cm^{-2} s^{-1} is expected, and a total integrated luminosity of 10 to 15 fb^{-1} will be accumulated by 2009. For operations at such a high luminosity, CDF needs further upgrades of some of the detector components. They include the replacements of the silicon detector and the central preshower detector. R&D efforts for the upgrades are already under way, and the Japan group has started making significant contributions.

In the remainder of this report we summarize physics results and prospects in Run IIa, and detector upgrade efforts for Run IIa/b, with an emphasis on contributions from the Japan group.

1 Physics Results and Prospects in Run II

We expect a data sample corresponding to an integrated luminosity of 2 fb^{-1} in Run IIa. This means a twenty-fold increase in the amount of data over the previous run, Run I. Also, the Tevatron beam energy has been increased to give a center-of-mass energy of 1.96 TeV.

We plan on carrying out a broad physics program, and preliminary results have already emerged from Run-II data. We describe some of them below, along with prospects with full 2 fb^{-1} of data.

1.1 Top quark properties

Since the top quark was discovered by CDF in 1995, tens of pair-produced top quark events were reconstructed and a various measurements of their properties were performed in a data sample of 110 pb^{-1}. However, most of the measurements were statistically limited, given the relatively small number of the reconstructed events. Therefore, all measurements are expected to improve with the increased amount of data in Run II.

The top analysis with Run-II data has thus far concentrated on measurements of the mass and production cross section. The production cross section has been measured using both lepton + jet and di-lepton channels. A candidate event in the lepton + jet channel is shown in Figure 3, where two b-jets are identified by secondary vertex tags. The jet multiplicity distribution of the W + n-jet events is shown in Figure 4, where the excess over expected background in $n = 3$ and $n \geq 4$ bins is explained by the contributions from the top quark. The $t\bar{t}$ production cross section is measured to be $\sigma = 5.3 \pm 1.9$ (stat) $\pm$ 0.8 (syst) $\pm$ 0.3 (lum) pb (Figure 5). K. Sato (Tsukuba) has contributed to the analysis, in particular the calculations of event acceptance, while S. Tsuno (Tsukuba) has provided new Monte Carlo event generation techniques for $W + n$-jet production. The corresponding cross section from the di-lepton channel is $\sigma = 13.2 \pm 5.9$ (stat) $\pm$ 1.5 (syst) $\pm$ 0.8 (lum) pb. They both are in agreement with a next-to-leading order QCD calculation of $6.7^{+0.71}_{-0.88}$ pb for $m_{\rm top} = 175$ GeV/c^2. The top quark mass is extracted from the lepton + jet channel to be $m_{\rm top} = 171.2 \pm 13.4$ (stat) $\pm$ 9.9 (syst) GeV/c^2, which is shown in Figure 6.

With 2 fb^{-1} of data the mass will be measured with a precision of about 3 GeV/c^2 [1, 2], and $t\bar{t}$ production cross section with a precision of 9%. Other production and decay properties will be also measured precisely, including $t\bar{t}$ spin correlations and $W^{\pm}$ boson helicity. Single top quark production should be observed, allowing a direct measurement of the partial width $\Gamma(t \to W^+ b)$ and a determination of CKM matrix element $|V_{tb}|$ to 13%. Also, searches will be performed for new particles such as a charged Higgs boson through the top decay $t \to H^+ b$, and new resonance states decaying into $t\bar{t}$ pairs.

1.2 Electroweak physics

Studies of single gauge boson production continue, at a new center of mass energy of 1.96 TeV. Clean signals of $W^+ \to \ell^+\nu$ and $Z^0 \to \ell^+\ell^-$ decays have been observed in Run-II data. Figure 7 shows a transverse mass distribution of the electron and missing transverse energy system for $W^+ \to e^+\nu$ candidates. Figure 8 shows an invariant mass distribution for $Z^0 \to e^+e^-$ candidates. The production cross sections are measured to be $\sigma(\bar{p}p \to W^\pm X) \cdot \mathcal{B}(W^\pm \to \ell^\pm\nu) = 2.64 \pm 0.01$ (stat) $\pm$ 0.09 (syst) $\pm$ 0.15 (lum) nb and $\sigma(\bar{p}p \to Z^0 X) \cdot \mathcal{B}(Z^0 \to \ell^+\ell^-) = 267.0 \pm 6.3$ (stat) $\pm$ 15.2 (syst) $\pm$ 16.0 (lum) pb, respectively. They are illustrated in Figure 9 as a function of the center-of-mass energy together with earlier measurements at Tevatron and CERN. The values at 1.96 TeV are roughly 9% higher than at 1.8 TeV.

With 2 fb^{-1} of data the $W^\pm$ boson mass will be measured with a precision of about 30 MeV/c^2. Combined with top quark mass measurements, it will provide constraints on the Higgs boson mass with a relative precision of 30%. This is illustrated in Figure 10 [1].

Another area of study concerns the pair production of gauge bosons. The unified electroweak theory has a non-Abeian nature in its gauge structure, resulting in self-couplings among gauge bosons such as $W^+W^-Z^0$ and $W^+W^-\gamma$ vertices. Production of $W^\pm\gamma$ pairs is studied. 44 (38) candidates with photons above 7 GeV/c have been observed in the $W \to e\nu$ ($\mu\nu$) channel among 72 pb^{-1} of data. Photon transverse momentum distribution is shown in Figure 11, which is consistent with standard model predictions. N. Tanimoto (Okayama) has performed the muon channel analysis. More detailed studies of self-couplings of the electroweak gauge bosons will be performed, including radiation amplitude zero in $W^\pm\gamma$ production.

1.3 Bottom and charm physics

Traditionally CDF relied on leptons to trigger on and collect decays of B hadrons, such as $\bar{B} \to \ell^-\bar{\nu}X$ and $B \to J/\psi X \to \ell^+\ell^- X$. In Run II, CDF has introduced a device called SVT, which uses information from the silicon vertex detector at the second level of the trigger and calculates impact parameter of charged tracks with about 50 μm precision for $p_T > 2$ GeV/c. It enables us to collect decay products of long-lived particles such as B and charm hadrons. An example of signals from this new trigger system is shown in Figure 12. A huge signal of 450 k events has already been obtained in a data sample corresponding to 65 pb^{-1}, and thus charm physics has become a new area of physics investigations at CDF. An analysis on relative branching fractions $\mathcal{B}(D^0 \to K^-\pi^+)$, $\mathcal{B}(D^0 \to K^+K^-)$ and $\mathcal{B}(D^0 \to \pi^+\pi^-)$ has been performed. A search for a FCNC decay $D^0 \to \mu^+\mu^-$ has produced an upper limit $\mathcal{B}(D^0 \to \mu^+\mu^-) < 2.4 \times 10^{-6}$ (90% CL), already surpassing the PDG 2002 value. Searches for lifetime differences and CP violation are planned for the $D^0\overline{D}^0$ system.

One of the CDF B physics goals is to observe $B_s^0\overline{B}_s^0$ oscillations and measure its frequency

Δm_s. It should provide a clean determination of the Cabibbo-Kobayashi-Maskawa matrix elements $|V_{td}/V_{ts}|$. CDF plans to use fully reconstructed decays collected by SVT so as to allow precise determination of B_s^0 meson momentum on an event-by-event basis. Such signals have also been observed, which are shown in Figure 13. In addition, two-body decays of B^0 mesons to light pseudoscalars are observed (Figure 14). The signal peak is a mixture of four decay modes: $\overline{B}^0 \to K^-\pi^+$, $\overline{B}^0 \to \pi^+\pi^-$, and $\overline{B}_s^0 \to K^+K^-$, $\overline{B}_s^0 \to K^+\pi^-$. The composition will be determined using dE/dx information from the central drift chamber. Measuring CP violation in $B^0/\overline{B}^0 \to \pi^+\pi^-$ and $B_s^0/\overline{B}_s^0 \to K^+K^-$ modes simultaneously may allow a clean determination of the CKM phase γ [3].

Lepton triggers still remain effective and useful channels for B physics. Figure 15 shows a $J/\psi \to \mu^+\mu^-$ signal from Run-II data. Thanks to a lowered p_T threshold on muons, J/ψ yield per unit amount of data is a factor of two higher than in Run I. Various B-hadron signals such as $B^+ \to J/\psi K^+$, $B^0 \to J/\psi K^{*0}$, $B^0 \to J/\psi K_S^0$, $B_s^0 \to J/\psi\,\phi$ and $\Lambda_b^0 \to J/\psi\,\Lambda^0$ have been observed and are used to measure their masses, lifetimes and relative branching fractions. T. Yamashita (Okayama) has been working on $\Lambda_b^0 \to J/\psi\Lambda^0$ measurements. Single leptons are a good source of semileptonic B decays. S. Uozumi (Tsukuba) has been a major contributor in this area, demonstrating signals such as $\overline{B} \to \ell^-\bar{\nu}D^0X$, $\overline{B} \to \ell^-\bar{\nu}D^{*+}X$, and $\overline{B}_s^0 \to \ell^-\bar{\nu}D_s^+X$. Their lifetimes and lifetime differences will be measured with high precision with the sample. Also, $B_s^0\overline{B}_s^0$ oscillations with a modest value of Δm_s can be looked for.

1.4 Quantum chromodynamics

A wide variety of measurements will be performed at a new center-of-mass energy of 1.96 TeV. Also, increased statistics allow measurements in a wider range of spectra, e.g. highest E_T jets, photons and other objects, and with less statistical uncertainties. They will serve as precision tests of perturbative QCD calculations.

An example is a measurement of inclusive production of jets. Figure 16 shows a measurement of inclusive jet production in various rapidity ranges. Figure 17 shows a ratio of jet production cross sections at $\sqrt{s} = 1.96$ TeV (Run II) and 1.8 TeV (Run I). Increased sensitivity at the high E_T end of the spectrum is obvious. Another example is production of J/ψ's. In Run I, CDF found a surprisingly high rate of direct production of J/ψ's, fifty times higher than theory [5]. The lowered muon trigger threshold has provided a reasonable acceptance down to $p_T^{J/\psi} = 0$ (Figure 18). The production cross section is measured as a function of $p_T^{J/\psi}$ and is shown in Figure 19. The value integrated over p_T and rapidity $|y| < 0.6$ is $240 \pm 1\,^{+35}_{-28}$ nb. T. Yamashita has contributed to this analysis. The sample should also allow a better measurement of production polarization, which is very useful in discriminating various production mechanisms, such as gluon fragmentation and color octet models.

1.5 New particle searches

Searches for the Higgs boson, supersymmetric particles and other new particles will be performed. The standard model Higgs boson can be searched for in a mass range up to 120 GeV/c^2 with 2 fb^{-1} of data [4]. This is shown in Figure 20. For a low mass Higgs, production in association with a gauge boson $W^{\pm}$ or Z^0 will be the most sensitive mode. The Higgs boson will decay predominantly to a $b\bar{b}$ pair in this mass region. At a high mass, around 150 GeV/c^2 or above, the decay to W^+W^- and Z^0Z^0 pairs will provide a very distinctive signature and our sensitivity is pretty high. In the intermediate mass region, associated production $\bar{p}p \to W^{\pm}HX$ followed by a Higgs decay into a virtual or real W boson pair $H \to W^{(*)+}W^{(*)-}$ provides a final state consisting of three W bosons in the event. Two of them always have the same charge, and it is also the case for their decay leptons. It is a very distinctive signature. If all three W bosons decay leptonically, it provides a even cleaner signal.

Many extensions of the standard model require extra U(1) gauge group and thus a new gause boson similar to Z^0. CDF has looked for such Z' bosons in their decay to $\ell^+\ell^-$. Figure 21 shows an e^+e^- invariant mass spectrum from Run-II data, which is described by contributions from known sources. A lower limit of 665 GeV/c^2 is placed assuming the standard model couplings of Z'. K. Ikado (Waseda) has performed the analysis.

Y. Miyazaki (Osaka City) performed using Run-I data a search for the pair production of scalar top quarks that subsequently decay, violating R-parity, into a tau lepton and a bottom quark [6]. The tau lepton is identified with its decay into one- and three-prong hadrons. The method is demonstrated by reconstructing the decay $Z^0 \to \tau^+\tau^-$, where one of the tau decays semileptonically into an electron or a muon, and the other tau decays hadronically. The charged multiplicity is used to identify hadronic decays of tau. The scalar quark is looked for with a final state consisting of an electron, a tau and two b-quark jets. No candidate event is found with an expected background of 1.92 ± 0.18 events. An upper limit on the production cross section has been placed, and a lower limit on the squark mass of 111 GeV/c^2 is obtained at 95% C.L.

2 Detector Upgrades for Run II

2.1 Plug upgrade calorimeter

A new, scintillator-based plug calorimeter [7] has been constructed and installed in the CDF detector. The analysis of Run-II data is in progress, in order to evaluate overall performance of the calorimeter such as calibration of the energy scale. Also, efforts have been made to establish off-line reconstruction algorithms for the identification of electrons and photons in the plug region.

Y. Seiya and S. Uozumi from Tsukuba have contributed to the plug calorimeter efforts.

Y. Seiya was a co-leader for the plug calorimeter project.

2.2 Silicon detectors: SVX II and ISL

The Silicon Vertex Detector (SVX II) and the Intermediate Silicon Layers (ISL) will provide precision charged particle tracking essential for detection of long-lived particles such as B hadrons. The construction of the both detectors had been complete, and they were installed inside the CDF detector in February 2001. Since then they were gradually integrated into CDF for readout, and presently more than 90% of all the channels are functioning (Figure 22).

The production of double-sided silicon micro-strip sensors for SVX II had been completed previously. The sensors for the Layer 3 of SVX II were assembled into quarter-ladders at Hamamatsu Photonics. They were tested for electrical connections to hybrid readout electronics and for dead channels. T. Ohsugi, Y. Iwata (Hiroshima), I. Nakano, R. Tanaka, N. Tanimoto, T. Yamashita (Okayama), and R. Takashima (Kyoto University of Education) have been working on the SVX II project.

K. Hara, M. Shimojima and Y. Takeuchi from Tsukuba have worked on the silicon sensors of the ISL detector. The production of double-sided silicon micro-strip sensors was completed at Hamamatsu. Sampling probing tests were performed to assure quality, including $I-V$ characteristics, leakage current, and dead channel fraction. T. Okusawa, T. Yoshida (Osaka City) and Y. Kato (Kinki) have worked on the data acquisition system used for testing hybrids.

Y. Takeuchi, S. Tsuno (Tsukuba), N. Tanimoto and T. Yamashita have developed a system for monitoring the silicon detectors. An example is shown in Figure 23.

2.3 Data acquisition system and monitoring

M. Shimojima (Nagasaki) and H. Matsunaga (Tsukuba) have assumed responsibility for the consumer-server/logger system, which, as part of the online data acquisition system, receives events from the level-3 trigger and sends to disk and tape storage devices as well as to online monitoring programs. T. Arisawa and K. Ikado (Waseda) are responsible for the monitoring programs that check detector performance and data quality. Both of these systems have been operational smoothly in Run II.

A. Miyamoto and Y. Fujii (KEK) have contributed to the event display program, in particular the central calorimeter wedge display.

2.4 Time-of-flight detector (TOF)

The TOF detector is a set of scintillation counters that provides K/π separation up to 1.6 GeV/c in momentum. K. Sato and F. Ukegawa (Tsukuba) were in charge of production and

quality control of photomultiplier tubes. The tubes have been tested at KEK for performance in a 1.4-T magnetic field, sent to FNAL, and installed in the CDF detector. The construction of the TOF detector itself was completed in 2000, and the installation of readout electronics was completed by summer 2001. All channels are read out and calibrations have been carried out using collision data [8]. K. Sato has performed a measurement and equalization of PMT gains, achieving a uniform response among different channels. He has also studied long term stability of gains using collision data. Figure 24 shows mass distributions for $\phi \to K^+K^-$ candidates before and after applying kaon identification cuts using TOF information. The signal-to-noise ratio improves by a factor of 20 while keeping 82% of the signal. It demonstrates that the detector is ready for use in physics analyses. F. Ukegawa was a co-leader of the TOF project.

2.5 Silicon detector upgrade for Run IIb

Inner layers of the SVX II detector will need to be replaced because of radiation damage they suffer from once CDF accumulates an integrated luminosity of about 5 fb^{-1} [9]. The R&D efforts for the replacement have already been started. The solution chosen by CDF is to use single-sided sensors that can be operated at higher bias voltages than present double-sided sensors. To simplify construction, all layers consists of a single, identical unit called a stave (Figure 25). K. Hara, S. Aoki and S. Takei (Tsukuba) have addressed issues such as cooling, support structure and the amount of material. I. Nakano (Okayama) has started development of high density, printed-circuit flat cables for readout for Layer 0. In 2002 prototype sensors have been produced and tested for characteristics such as leakage current and capacitance. Some are irradiated to neutrons and tested afterward. They have been found to satisfy our requirements, and the production has started.

K. Hara is a co-leader of the Run-IIb silicon project.

2.6 Central preshower detector upgrade for Run IIb

The central preshower detector (CPR) is located behind the CDF solenoid (about one radiation length thick) and before the central electromagnetic calorimeter CEM. It samples electromagnetic showers at their early development stage, and plays important roles in identification of electrons and photons.

The current CPR detector is a slow gas chamber with relatively coarse segmentation. This detector will suffer a serious occupancy problem once the Tevatron luminosity exceeds 10^{32} cm^{-2} s^{-1}. The solution will be to replace it with a fast, finely-segmented device. Our present choice is to use plastic scintillator with a wavelength shifting fiber for readout, similar to the preshower detector (PPR) for the upgraded plug calorimeter.

Photons will be read out with a photomultiplier tube. A total number of channels of 3072 is envisioned, and the plan is to use multi-anode PMTs to reduce cost. The current choice

is Hamamatsu H8711A-10MOD (R5900-00-M16). This tube has 16 pixels with a pixel size of 4 mm $\times$ 4 mm. We would need 64 channels (four tubes) per CEM wedge, with a total of about 240 tubes including spares.

In 2002 we tested 10 prototype tubes and examined the characteristics in terms of anode uniformity, pulse linearity, absolute gains, cross talk, magnetic field effects and so on. Anode uniformity of 10% is observed among different pixels within a tube. It has been decided to use a tapered base circuit so as to keep a good pulse linearity for large pulses. The design was finalized, and the production has started.

References

[1] "The CDF II detector, Technical design report",
CDF II Collaboration, Fermilab-Pub-96/390-E (1996).

[2] "Review and preview of top physics at CDF", R. Roser, CDF Collaboration,
talk at the Thinkshop, top-quark physics for Run II, Fermilab, November 10 - 12, 1998.

[3] "B Physics at the Tevatron : Run II and Beyond",
K. Anikeev *et al.*, hep-ph/0201071 (2002).

[4] "Report of the Higgs Working Group of the Tevatron Run II SUSY/Higgs Workshop",
M. Carena, J. S. Conway, H. E. Haber, J. D. Hobbs, hep-ph/0010338 (2000).

[5] "J/ψ and $\psi(2S)$ Production in $p\bar{p}$ Collisions at $\sqrt{s} = 1.8$ TeV",
CDF Collaboration, F. Abe *et al.*, Phys. Rev. Lett. **79**, 572 (1997).
"Production of J/ψ from χ_c Decays in $p\bar{p}$ Collisions",
CDF Collaboration, F. Abe *et al.*, Phys. Rev. Lett. **79**, 578 (1997).

[6] "Search for Scalar Top Quark Pair-Production by R-Parity Violating Decay Mode in $p\bar{p}$ Collisions at $\sqrt{s} = 1.8$ TeV,
Y. Miyazaki, Ph. D. Thesis, Osaka City University, 2002.
CDF Collaboration,
http://www-cdf.fnal.gov/physics/exotic/run_1b_rpv_stop_e/public.html

[7] "The CDF Plug Upgrade Electromagnetic Calorimeter: Test Beam Results",
M. Albrow, T. Asakawa, J. Iwai, S. Kim, Y. Seiya *et al.*,
Nucl. Instrum. Methods **A480**, 524 (2002).

[8] "The CDF-II Time-of-Flight Detector",
S. Cabrera, H. Kaneko,A. Kazama, S. Kim, K. Sato, K. Sato, F. Ukegawa *et al.*,
Nucl. Instrum. Methods **A494**, 416 (2002).

[9] "A Radiation Damage Test for Double-sided Silicon Strip Detectors",
Y. Iwata, T. Ohsugi, M. Ikeda, H. Kitabayashi, T. Ohmoto, R.Takashima *et al.*,
Nucl. Instrum. Methods **A489**, 114 (2002).

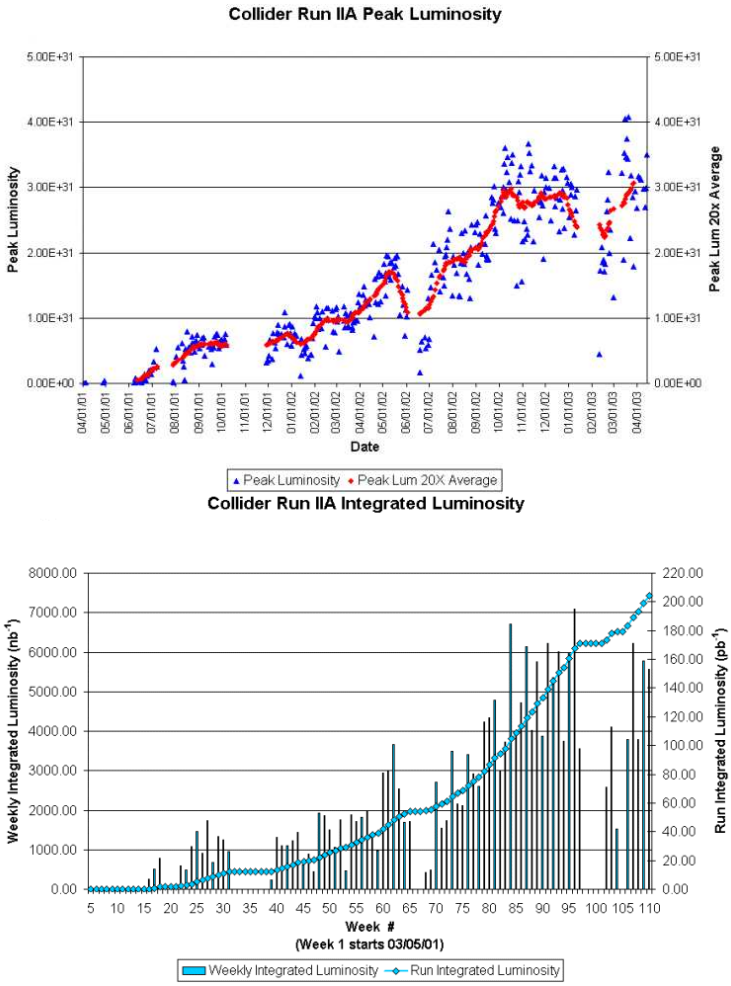

Figure 1: Tevatron performance in Run II. Top: instantaneous luminosity at the beginning of each store. Bottom: integrated luminosity delivered by week.

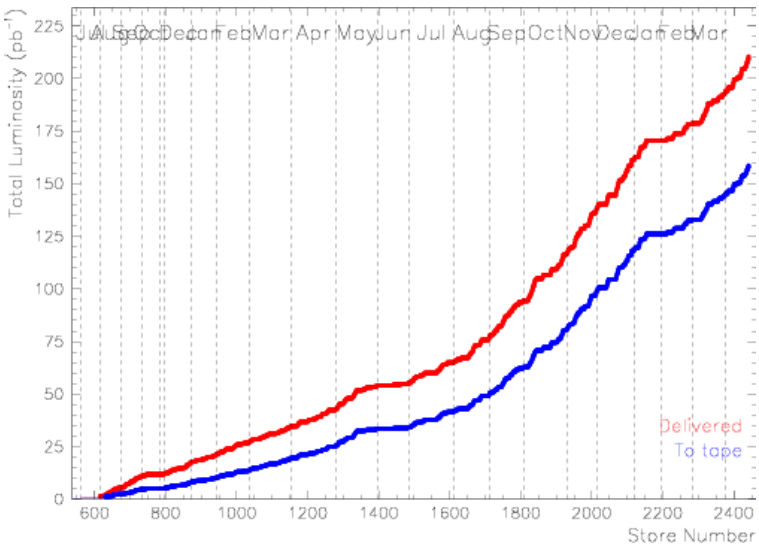

Figure 2: Integrated luminosity (top) delivered to and (bottom) recorded by CDF thus far in Run II.

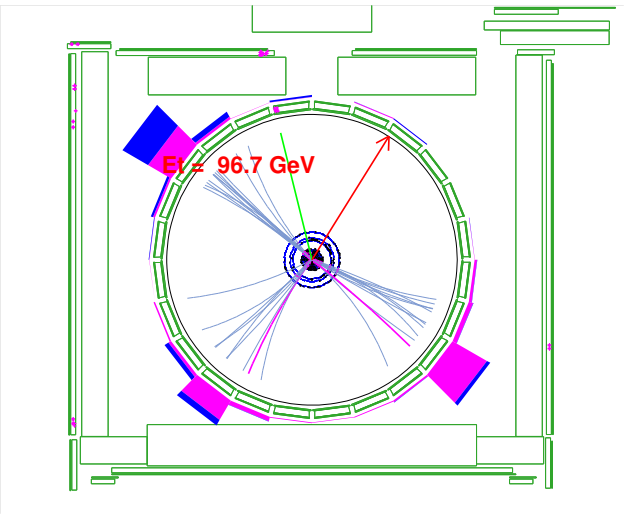

Figure 3: A top quark candidate event in the lepton + jet channel, where two b-jets are tagged by secondary vertices.

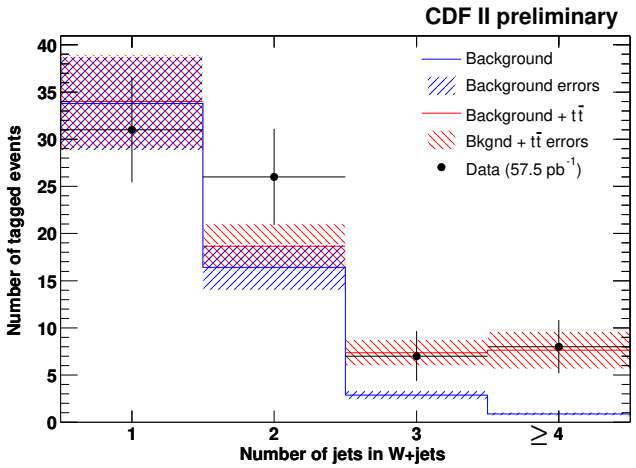

Figure 4: Multiplicity of jets in $W + n$-jet events.

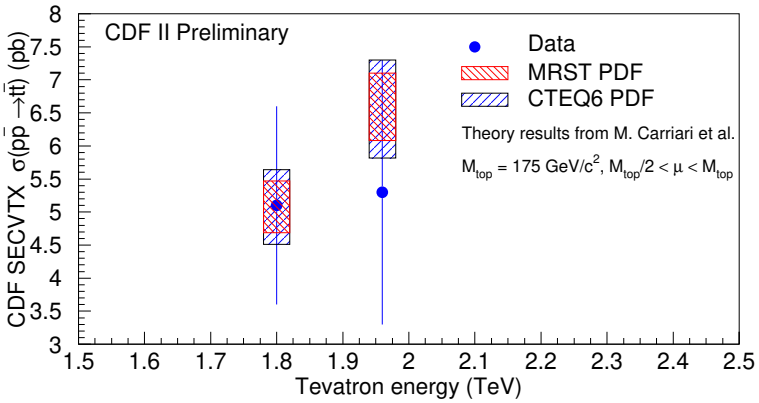

Figure 5: Top quark pair production cross section from the lepton + jet channel in Run II, with a comparison to theory and Run-I measurement.

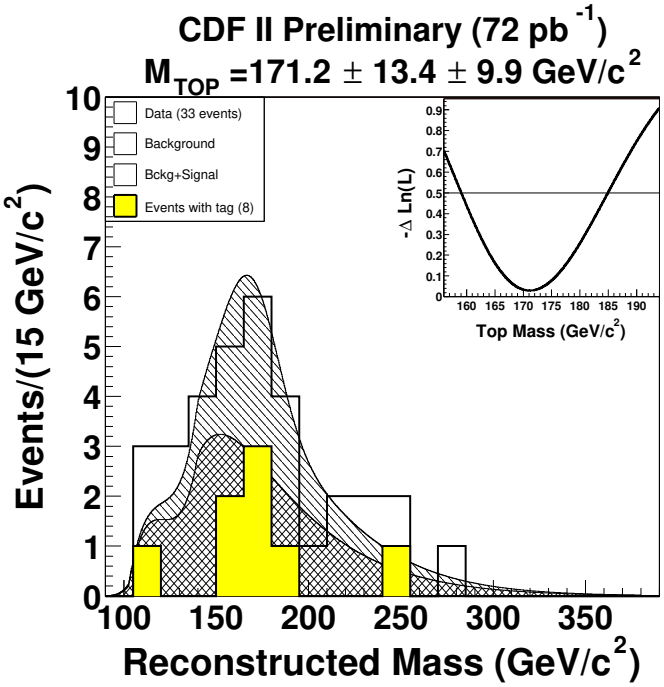

Figure 6: Top quark mass measurement from the lepton + jet channel in Run II. Inner histogram corresponds to events where one of the b-jets is tagged.

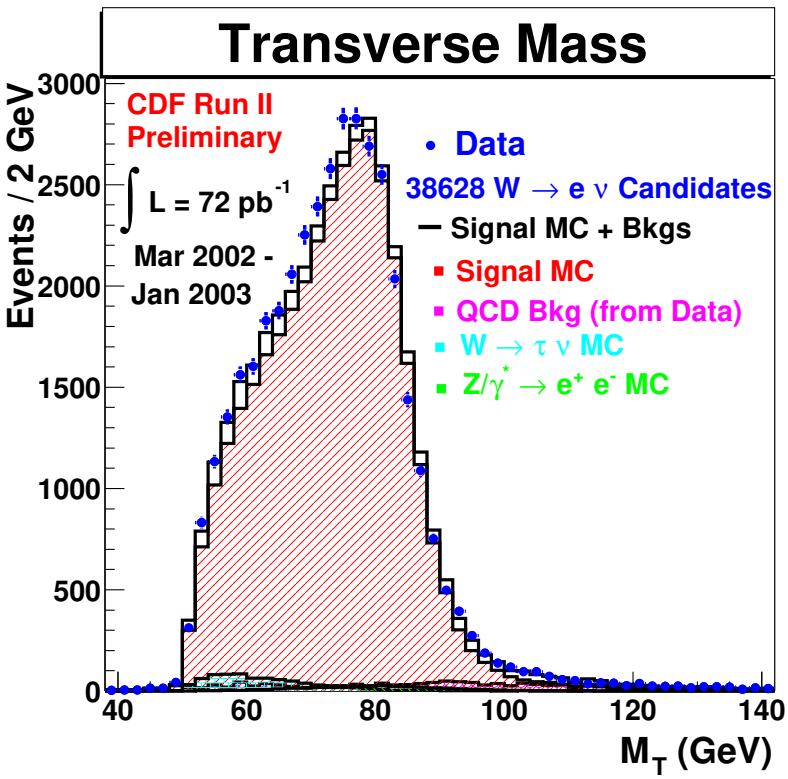

Figure 7: Transverse mass distribution of Run-II $W^+ \to e^+\nu$ candidates.

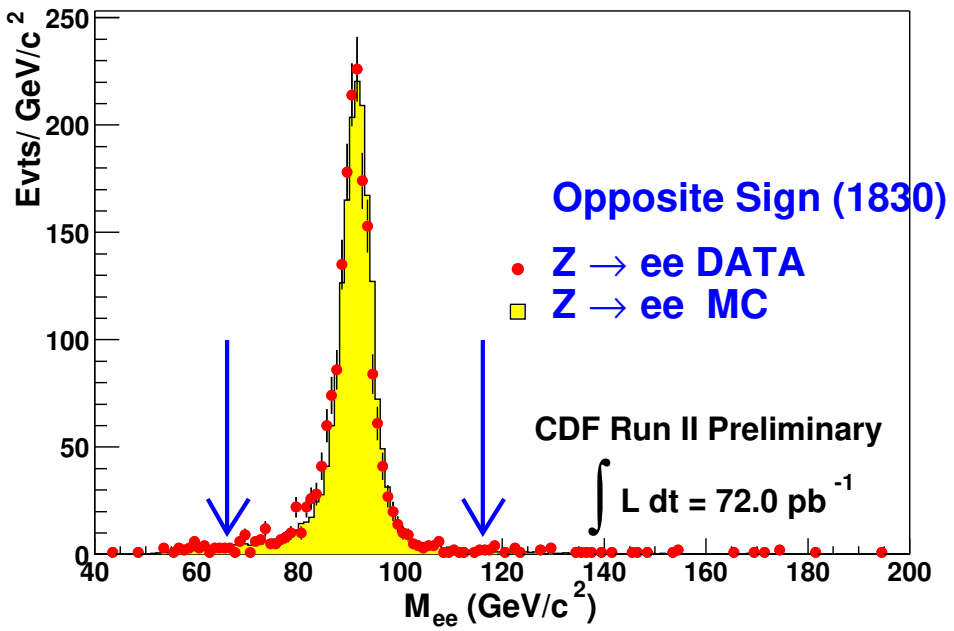

Figure 8: Invariant mass distribution of Run-II $Z^0 \to e^+e^-$ candidates.

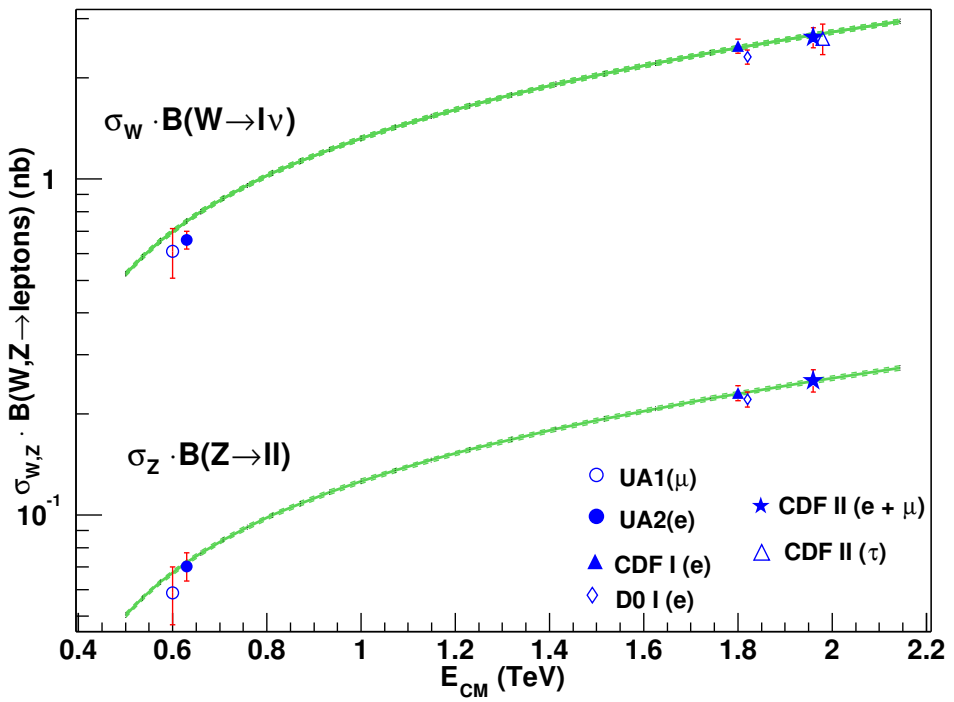

Figure 9: Production cross sections of $W^{\pm}$ and Z^0 bosons.

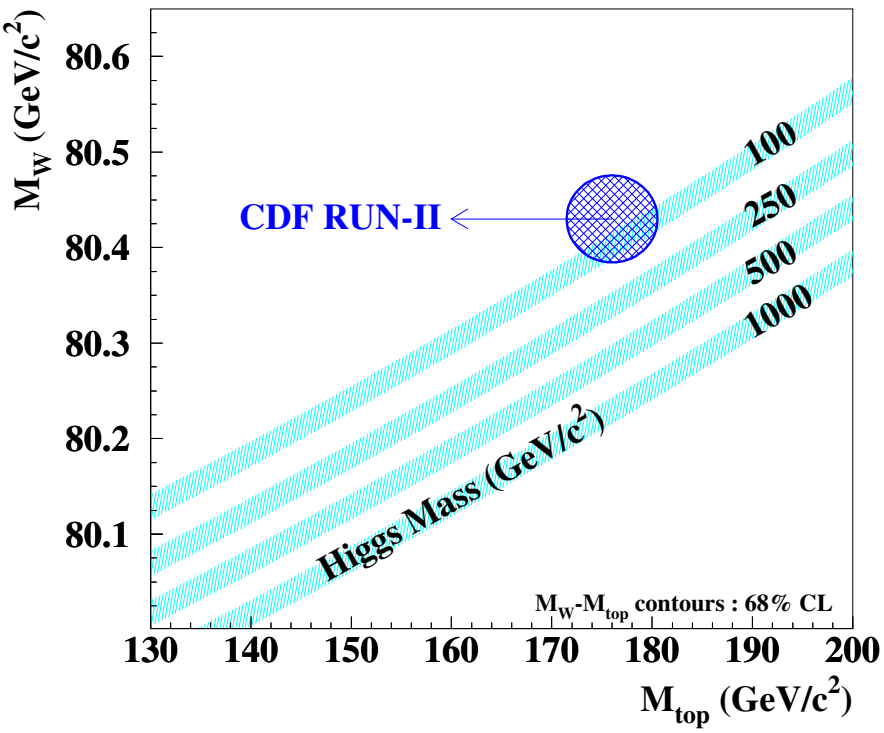

Figure 10: Expected precision in top quark and W boson mass measurements in Run II, and possible constraints on the Higgs boson mass.

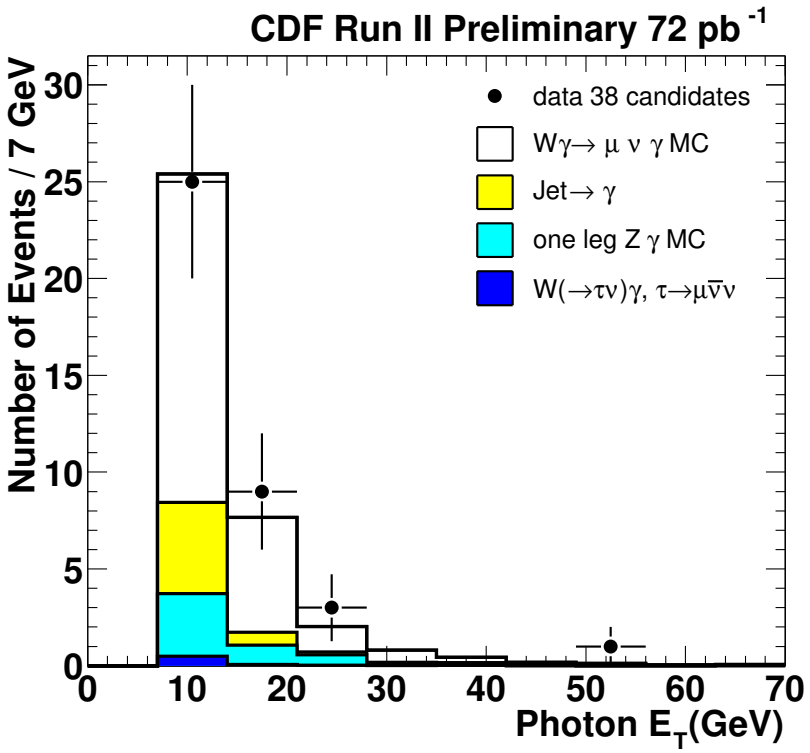

Figure 11: Photon transverse momentum distribution in $W\gamma$ pair production candidates.

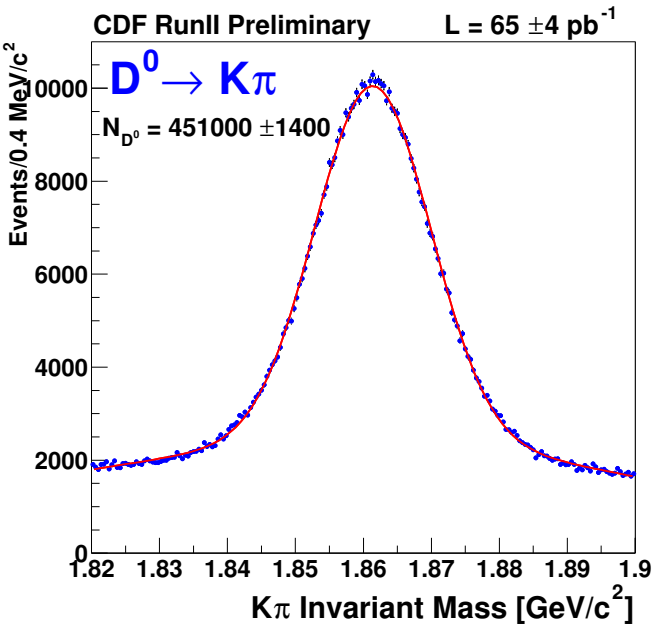

Figure 12: $D^0 \to K^-\pi^+$ signal reconstructed in a data sample collected using SVT trigger.

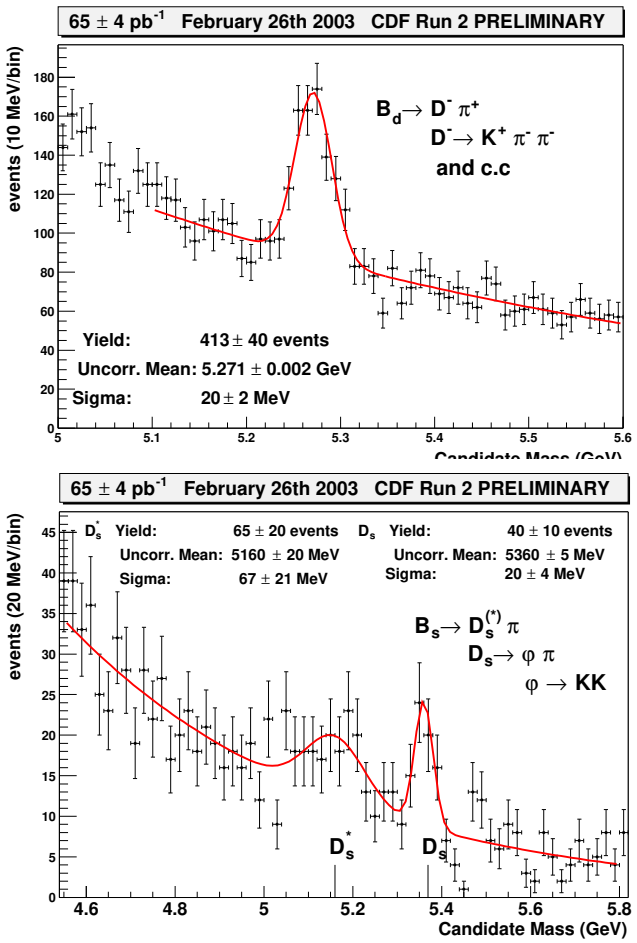

Figure 13: B meson signals from SVT trigger. Top: $\bar{B}^0 \to D^+\pi^-$, $D^+ \to K^-\pi^+\pi^+$. Bottom: $\bar{B}_s^0 \to D_s^+\pi^-$, $D_s^+ \to \phi\pi^+$.

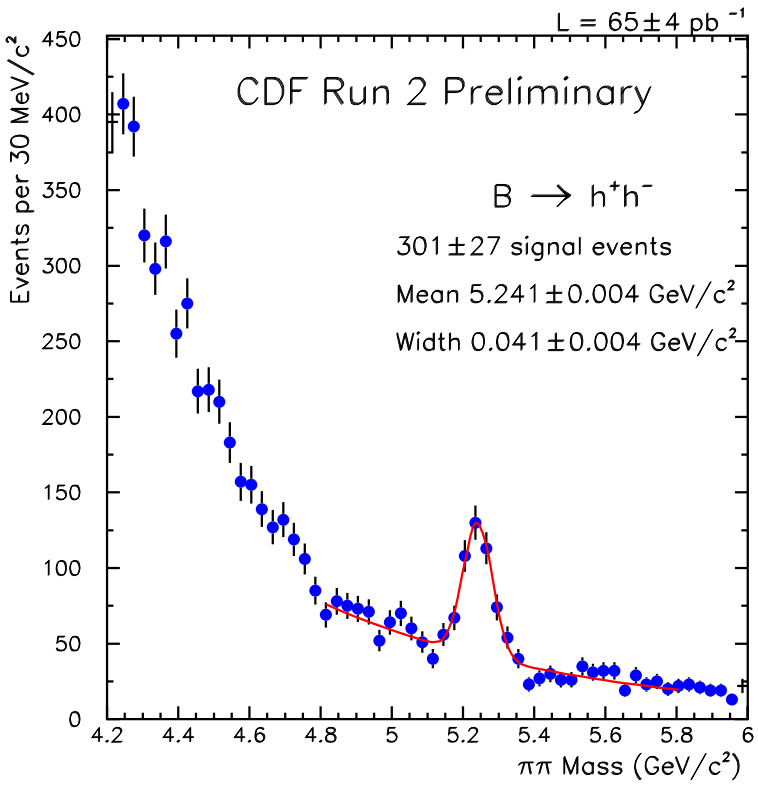

Figure 14: $B^0/B_s^0 \to h^+h^-$ signal from SVT trigger, where $h^\pm$ is either $\pi^\pm$ or $K^\pm$. Pion mass is assumed for reconstruction of two-body mass.

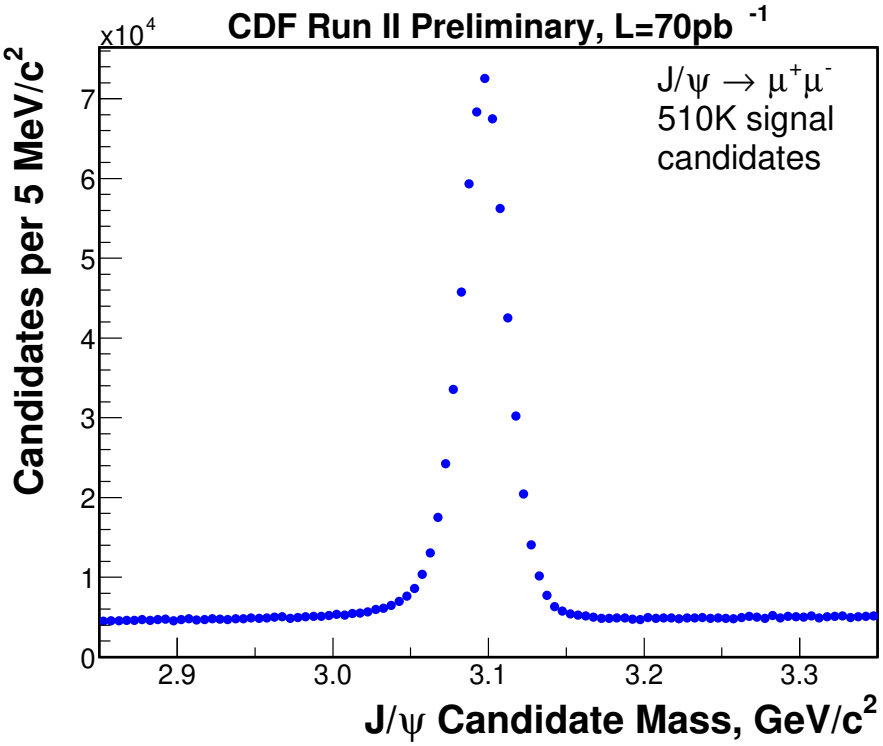

Figure 15: Run-II dimuon invariant mass distribution near J/ψ region.

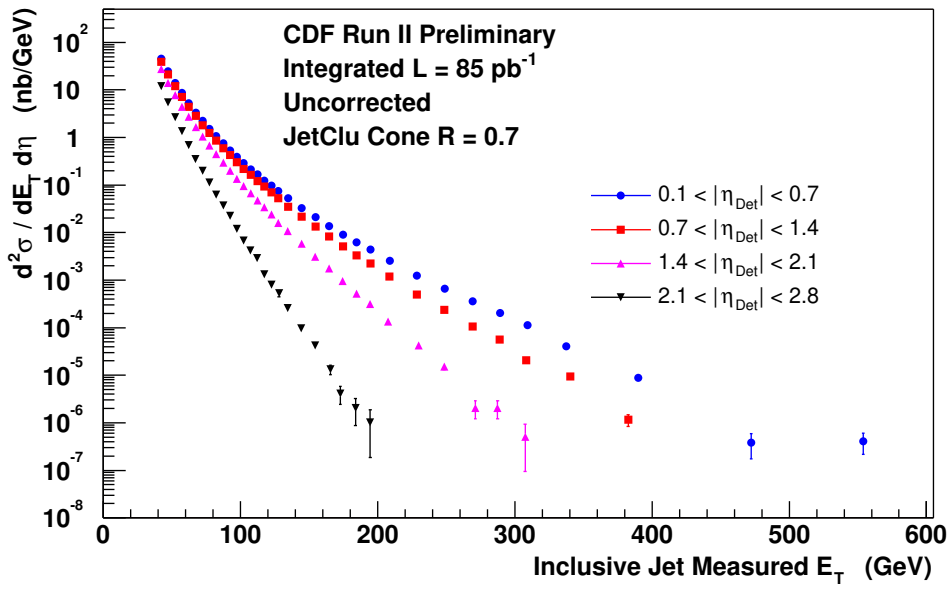

Figure 16: Run-II measurement of inclusive jet production in various rapidity ranges.

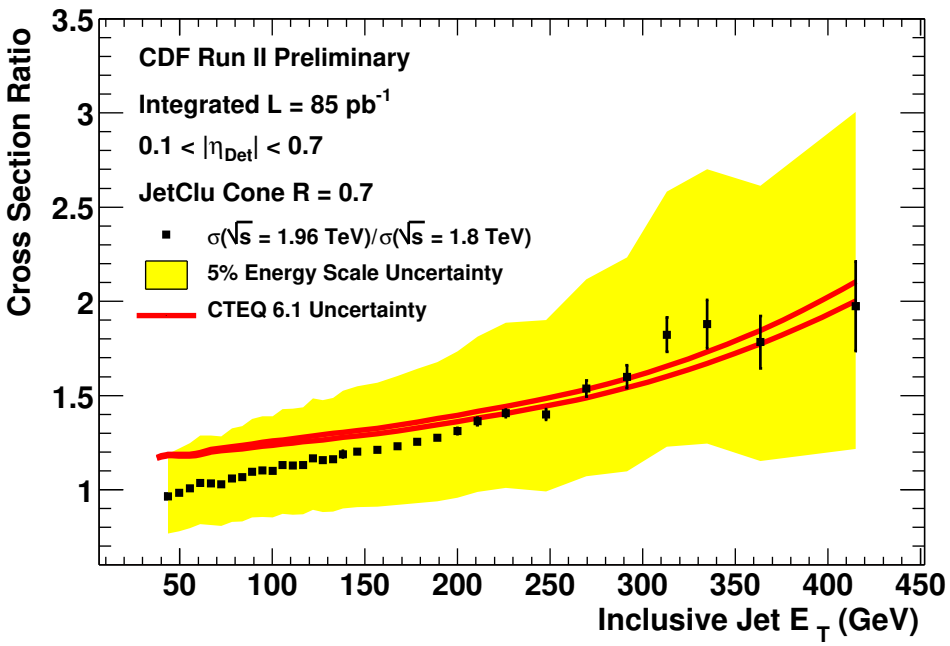

Figure 17: Ratio of inclusive jet production cross sections at $\sqrt{s} = 1.96$ TeV (Run II) and 1.8 TeV (Run I).

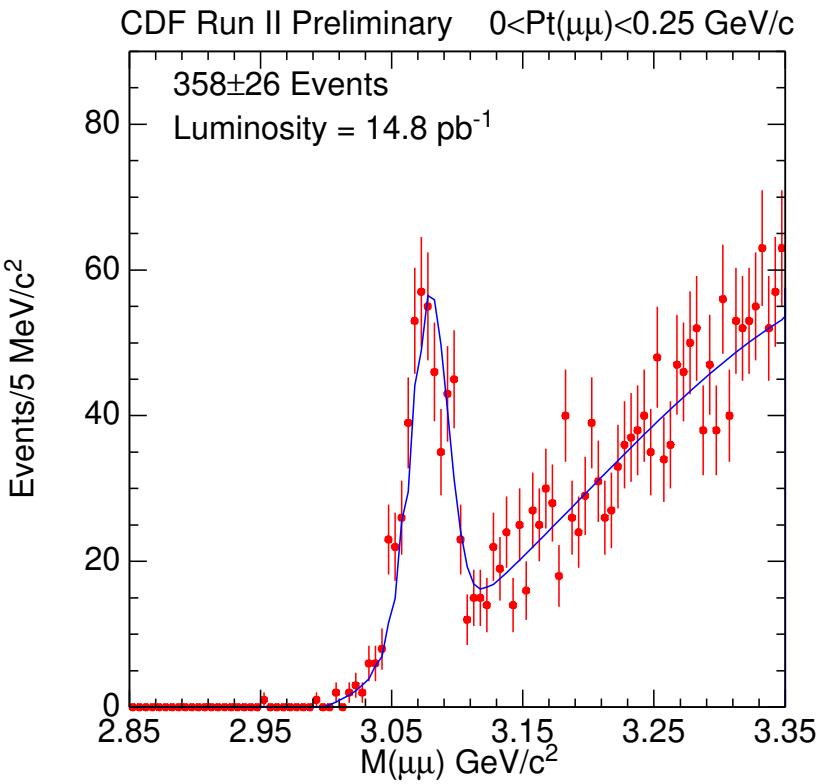

Figure 18: $J/\psi \to \mu^+\mu^-$ signal for the lowest p_T bin, below 0.25 GeV/c.

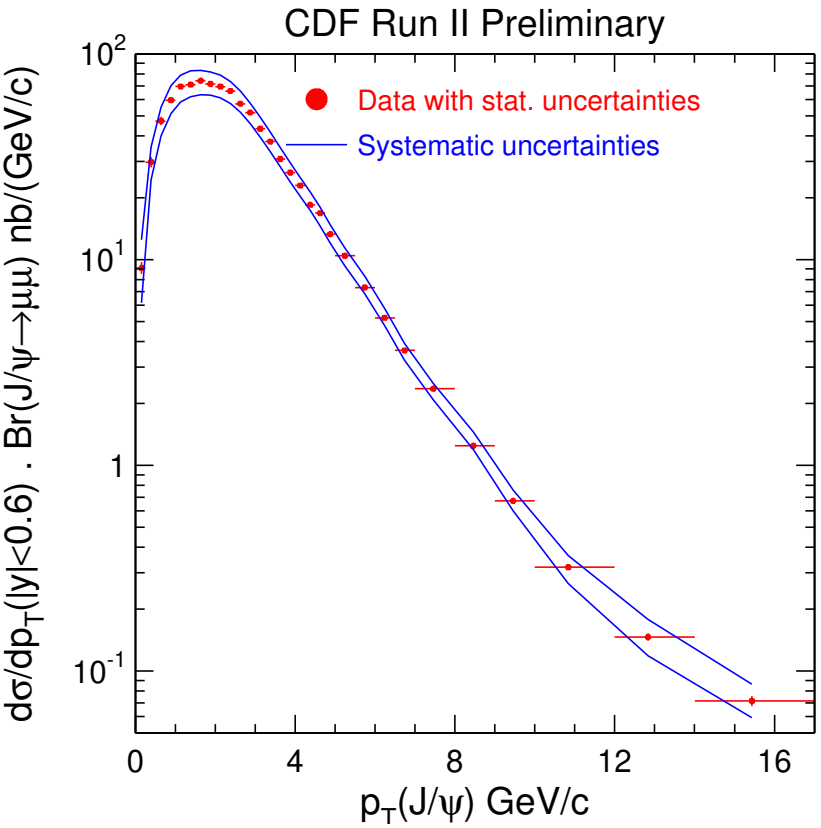

Figure 19: J/ψ production cross section from Run II.

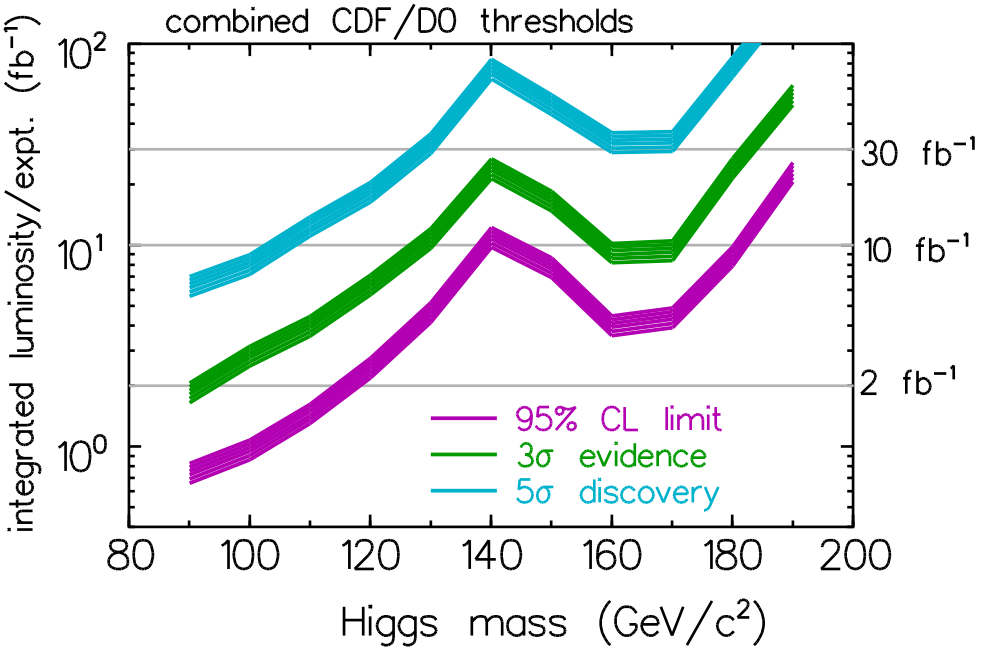

Figure 20: Tevatron reach for the standard model Higgs boson. Three bands show, as a function of the Higgs mass, the amount of data that are necessary (a) to exclude at 95% CL if the Higgs does not exist at that mass (bottom band), (b) to provide 3σ evidence for existence (middle), and (c) to discover with 5σ significance (top).

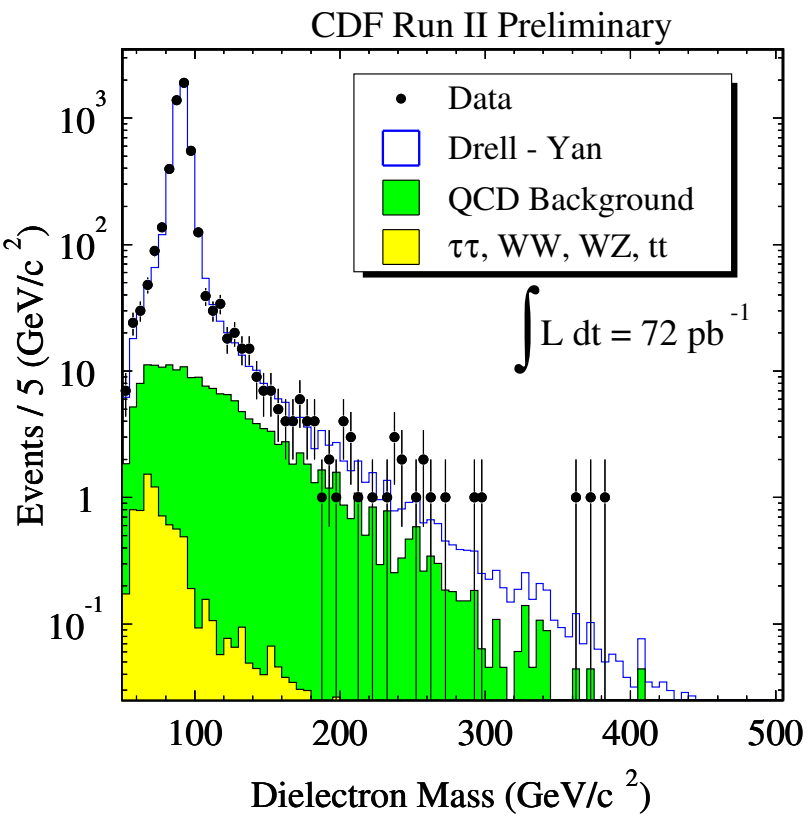

Figure 21: Invariant mass spectrum of e^+e^- pairs at high mass region.

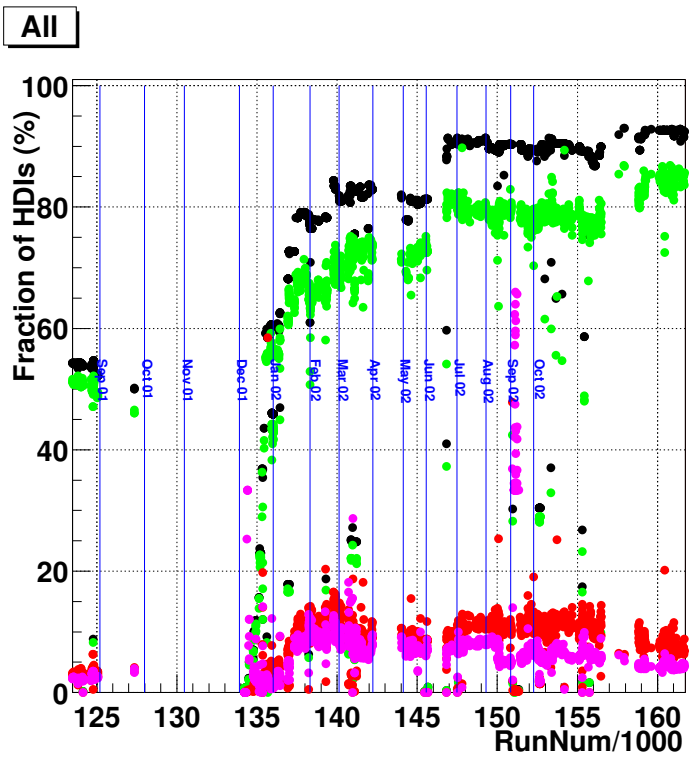

Figure 22: CDF-II silicon detector status. Fractions of channels read out are shown for combined Layer 00, SVXII and ISL detectors.

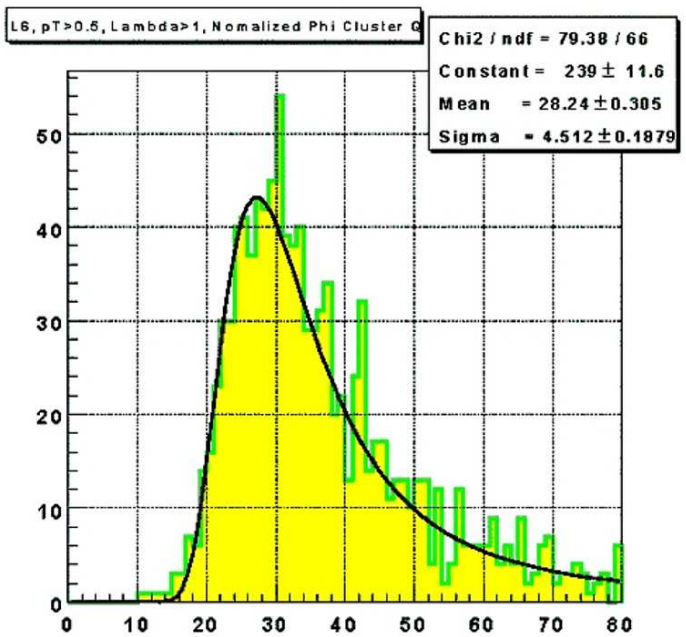

Figure 23: Pulse height distribution observed on ISL. A typical signal-to-noise ratio of 12 has been achieved.

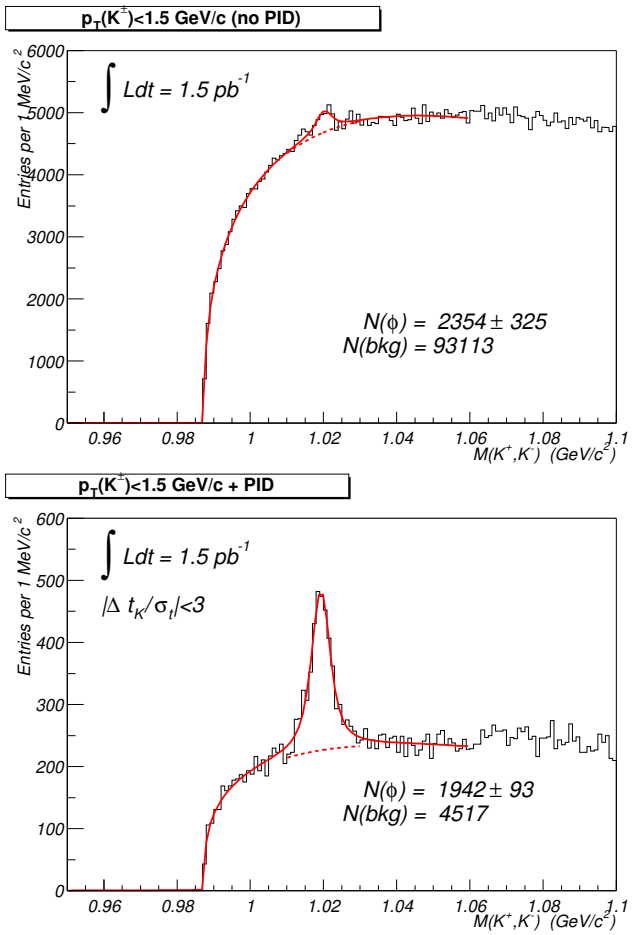

Figure 24: Invariant mass distribution of $\phi \to K^+K^-$ candidates before (top) and after (bottom) application of particle identification using TOF information.

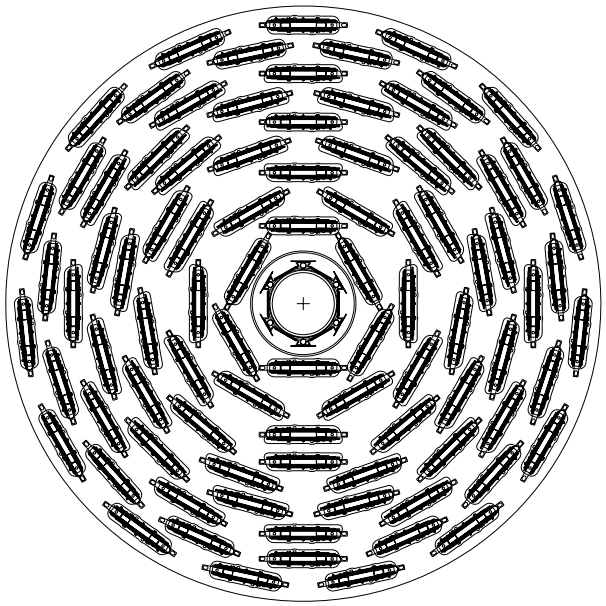

Figure 25: Layout of staves for CDF Run-IIb silicon detectors.